PHYSICAL REVIEW B VOLUME 25, NUMBER 10 15 MAY 1982

Finite-cluster description of electromigration

R. S. Sorbello
Department of Physics, University of Wisconsin-Milwaukee, Milwaukee, Wisconsin 53201

A. Lodder and S. J. Hoving
Natuurkundig Laboratorium, Vrije Universiteit, 1081 HV Amsterdam, The Netherlands
(Received 30 November 1981)

The problem of vacancy migration in a metal under the influence of an electric current is studied in several model situations. The wind force is calculated as a function of the position of the atom which moves towards the vacancy. A currently used model in pseudopotential calculations implies that plane waves are scattered by a potential which is found by subtracting the unperturbed lattice potential from the potential of the system with the vacancy. As soon as the atom has started to move the scattering potential in this "subtracted" model (SM) consists practically of two vacancies with the atom somewhere in between, which forms a cluster of three scatterers. Owing to neglect of the background lattice, the SM is bound to fail for strong scatterers. A new model is called finite cluster model (FCM). It allows for the treatment of stronger scatterers and the background lattice is accounted for depending on the size of the cluster. In this FCM the system is modeled by a finite cluster of atoms surrounding the vacancy. Results are obtained and discussed for the SM treated exactly which means that all multiple scattering effects are accounted for, and in the Born approximation. The FCM is treated exactly, for clusters containing 1, 3, 5, 7, 11, 15, and 19 atoms. The system treated has the fcc structure, the atomic potentials are represented by spherical wells, and in the results presented only s scattering is accounted for. The force in the region of interest appears to be largely reduced by the presence of an environment, particularly for stronger scatterers.

I. INTRODUCTION

When an electric field is applied to a metal a migration of atoms can be observed. This phenomenon, which is known as electromigration, is a subject of fundamental as well as technological interest.[1] Recent theoretical studies[2] essentially corroborate the traditional viewpoint[3] that the driving force for electromigration can be separated into two distinct contributions. One contribution is called the direct force and is due to the applied electric field $\vec{E}$ acting on the ion or atom of interest. For an ion of valence Z this force is $Ze\vec{E}$ where e is the charge of the proton. The second contribution to the driving force is called the wind force and arises from the current (or "wind") of electrons being scattered by the ion or atom of interest. The wind force is the subject of this paper. In particular, we shall evaluate the wind force within a finite-cluster model.[4] This will enable us to perform the first calculation of electromigration forces which includes multiple-scattering effects.

Multiple scattering of electrons during atomic migration is unavoidable: The region containing the migrating atom contains more than one scattering center and the electrons will suffer collisions with all of these centers. For example, in the case of interstitial migration, the scattering region, or defect complex, consists of the interstitial atom and the surrounding lattice distortion. In the case of vacancy migration, the defect complex consists of two nearest-neighbor vacancies with the migrating atom somewhere in between. Lattice distortion is also present. A realistic calculation of the wind force should allow for the scattering of electrons by the particular atomic configuration for the migration mechanism of interest.

Until now atomic configuration effects in electromigration have been treated only within lowest-order perturbation theory[5] or its equivalent in pseudopotential theory.[2,6,7] (A modified version of perturbation theory has been used in treating liquid metals.[8]) The perturbation theory or pseudopotential calculations are not expected to be valid when

any of the atoms in the defect complex is a strong scatterer (large phase shifts) or when the host metal is not free electron like. Furthermore, even for simple metals the phase shifts are not always small enough to allow one confidently to treat interstitials or vacancies as weak scatterers.[9] Thus, even for simple metals there is a real need to push the calculations beyond lowest-order perturbation theory and pseudopotential theory. For the case of electromigration in transition metals, it is even more important to consider the multiple-scattering aspects of the problem.

Recent theoretical work has led to an expression for the wind force in which multiple-scattering contributions are retained.[10,11] Denoting the wind force by $\vec{F}$, the result is

$$\vec{F}=-\sum_{\vec{k}} f_1(\vec{k}) \int |\psi_{\vec{k}}(\vec{r})|^2 \frac{\partial v_1}{\partial \vec{R}_1} d^3r \ , \tag{1}$$

where $f_1(\vec{k})$ is the perturbed electron-distribution function caused by the applied field and $\psi_{\vec{k}}(\vec{r})$ is the electron scattering wave function for an electron incident upon the defect complex. The interaction potential between an electron and the atom of interest is $v_1=v_1(\vec{r}-\vec{R}_1)$ where $\vec{R}_1$ is the position of that atom. The integration is over all space and the sum is over all electron states $\vec{k}$. The appearance of $f_1(\vec{k})$, however, limits the $\vec{k}$ summation to states on the Fermi surface. Expression (1) was explicitly obtained by Schaich[10] for a free-electron gas and is also consistent with force expressions derived by Sham[11] for the models he considered.

The derivation of expression (1) for a Bloch crystal is discussed in Sec. II. Here we only point out that Eq. (1) can be heuristically derived in an independent electron picture from the general Feynman-Hellmann[12] form for the force, i.e.,

$$\vec{F}=-\int n(\vec{r}) \frac{\partial v_1}{\partial \vec{R}_1} d^3r \ , \tag{2}$$

where $n(\vec{r})$ is the electron density. We can now argue that the electron density is simply the density appropriate to each scattering state summed over all the occupied scattering states. Since only the field-dependent part of the force is required, only the $f_1(\vec{k})$ part of the occupation is needed. That is

$$n(\vec{r})=\sum_{\vec{k}} f_1(\vec{k}) |\psi_{\vec{k}}(\vec{r})|^2$$

is to be used in Eq. (2). This immediately gives expression (1).

We remark that the force on an atom will in general depend on the coordinate $\vec{R}_1$ since $\psi_{\vec{k}}(\vec{r})$ in the vicinity of the ion depends on the detailed atomic configuration of the defect complex. The driving force for electromigration is the average of the actual driving force over the migration path, namely,

$$ZeE+L^{-1}\int \vec{F}\cdot d\vec{R}_1 \ ,$$

where the integral is over the path of length L. This average force times L equals the work done by the electron wind on the migrating atom. The work done, and hence the average force, is the quantity which influences the atomic migration.

Equation (1) is a powerful theoretical expression, but there are difficulties in applying it to realistic systems. One needs to know the distribution function $f_1(\vec{k})$ over the Fermi surface. Then one needs to perform the $\vec{k}$ integration over this generally complicated Fermi surface. The self-consistent electron-ion interaction v_1 is also required. Most difficult of all is the determination of the scattering states $\psi_{\vec{k}}(\vec{r})$.

Because of these difficulties no applications of Eq. (1) have been made for configurations of strong scatterers. Genoni and Huntington[13] have applied Eq. (1) for weak scatterers but have kept the Bloch-like character of the scattering state, i.e., they correctly evaluated $\psi_{\vec{k}}(\vec{r})$ to first order in v_1. They do, however, retain much of the complexity of the Fermi surface and of $f_1(\vec{k})$ even though their host metal Zn is nearly free electron like. Ideally one would like to go beyond this and introduce multiple scattering effects in $\psi_{\vec{k}}(\vec{r})$ while still retaining band-structure effects in $\psi_{\vec{k}}$ and $f_1(\vec{k})$. Here we settle for a more approximate treatment which still gives due emphasis on the multiple-scattering aspects of $\psi_{\vec{k}}(\vec{r})$ but is rather less faithful in describing the Bloch-like nature of $\psi_{\vec{k}}(\vec{r})$ or $f_1(\vec{k})$.

Our calculation is based on the finite-cluster model.[4] This model has previously been used in studies of densities of states[14] and of electron lifetimes[15] in metals and has been found to be useful. In this model $\psi_{\vec{k}}(\vec{r})$ is calculated by considering a plane wave incident on a finite cluster. The plane waves are assumed to be occupied according to the free-electron form of the distribution function $f_1(\vec{k})$. The multiple scattering within the cluster is solved exactly using Schrödinger's equation. The cluster consists of the migrating atom and the atoms in its neighborhood. As the cluster size increases one expects the calculation to become more

accurate, for a more representative portion of the host lattice is included in the evolution of $\psi_{\vec{k}}(\vec{r})$. To the extent that the finite-cluster wave function approaches the true wave function in the vicinity of the migrating atom, the form of Eq. (1) implies that the finite-cluster result should be a good approximation. Although certain details of $\psi_{\vec{k}}(\vec{r})$ and $f_1(\vec{k})$ are lost, especially when $\vec{k}$ is near a band edge, the $\vec{k}$-space summation in Eq. (1) is likely to reduce the importance of these lost details.

Our numerical calculations are restricted to *s*-wave scatterers in the geometry appropriate to the vacancy migration mechanism in a fcc metal. Cluster sizes of up to 19 atoms are considered. The emphasis here is on examining the multiple-scattering effects. Indirectly, this study provides a critical appraisal of pseudopotential calculations.[2,6] The present work should be regarded as a prelude to future calculations based on expression (1). Ultimately we would like to include *p*-wave and *d*-wave scattering in larger clusters and to calculate the alloy wave function $\psi_{\vec{k}}(\vec{r})$ more accurately.

In Sec. II we comment on the derivation of Eq. (1) for Bloch states and derive useful general expressions for determining $\vec{F}$ from cluster calculations. In Sec. III the finite-cluster model and its pseudopotential analogue (the "subtracted model") are discussed for the case of vacancy migration. Numerical results are presented and discussed in Sec. IV. Conclusions are stated in Sec. V. Atomic units are used such that $\hbar=2m=1$, where m is the electron mass.

II. EXPRESSION FOR THE WIND FORCE

Expression (1) for the wind force is a combination of Schaich's[10] Eqs. (29), (32), and (A1). It is the force on an ion at position $\vec{R}_1$, being part of a cluster of ions with potential

$$V(\vec{r})=\sum_i v_i(\vec{r}-\vec{R}_i)\ . \tag{3}$$

The deviation from equilibrium of the electron distribution $f_1(\vec{k})$ equals

$$f_1(\vec{k})=-e\tau\vec{E}\cdot\vec{v}\left[-\frac{\partial f_0(\epsilon-\epsilon_F)}{\partial\epsilon}\right], \tag{4}$$

τ being the transport relaxation time, $\vec{E}$ the applied electric field, $-e$, $\vec{v}$, and ϵ are the charge, velocity, and energy of an electron, respectively, ϵ_F is the Fermi energy, and f_0 is the Fermi-Dirac distribution function. Expression (1) was written down for a finite cluster immersed in a free-electron gas.

For our studies we would like to start from an expression which is valid in a solid as well, containing (1) as the free-electron limit. A first analysis for one migrating ion in a periodic solid which starts from a Kubo linear response theory formulation[16] as Schaich did for the free-electron gas, was given by Sham.[11] His formula (4.12) compared with Schaich's formula (33) suggests that (1) is valid for a cluster in a solid provided that $f_1(\vec{k})$ is the perturbed electron distribution function for the solid. This is equivalent to replacing τ in Eq. (4) by the generally anisotropic relaxation time $\tau(\vec{k})$ obtained by solving the Boltzmann equation. In fact, the reduction of the linear response expression for the wind force in a solid to the form (1) requires neglect of band-mixing contributions from nondiagonal matrix elements of the velocity operator. Sham neglects band-mixing contributions implicity by his treatment of the current vertex function,[17] and it is at this vertex that the distribution function $f_1(\vec{k})$ is effectively introduced. Accepting Sham's procedure, we find that the series generated by the diagrams in his Fig. 1 lead to the result given by our Eq. (1). We remark that Sham's analysis neglects certain vertex corrections and band polarization effects,[17] but these are usually small compared to the wind force.[2,17] These neglected terms can formally be regarded as corrections to the direct force $Ze\vec{E}$,[17] and are not of interest in the present study. We therefore regard (1) as a reliable expression for the wind force. We apply this expression to the finite cluster consisting of the migrating atom and the bulk atoms in its nearby environment. For simplicity, the anisotropy of $\tau(\vec{k})$ is ignored in our calculations.

In order to evaluate the expression for the wind force one needs the electron wave function in the range of the potential of the migrating ion. The treatment to be given is exact for a nonoverlapping muffin-tin potential. For sake of clarity we first write down the form of the wave function which is valid in the free-space region just outside the range of the potential at $\vec{R}_1$, using $\vec{x}$ as to be measured from $\vec{R}_1$ ($\vec{r}=\vec{x}+\vec{R}_1$)

$$\psi_{\vec{k}}(\vec{x}+\vec{R}_1)=\frac{4\pi}{\Omega^{1/2}}\sum_L i^l Y_L(\hat{k})\left[j_L(\vec{x}+\vec{R}_1)-i\sum_{\substack{j'L'\\ j''L''}} h^+_{L'}(\vec{x}+\vec{R}_{1j'})\,T^{j'j''}_{L'L''}J^{j''0}_{L''L}\right], \tag{5}$$

where Ω is the volume of the system, $j_L(\vec{r})=j_l(\kappa r)Y_L(\hat{r})$, j_l and n_l are the spherical Bessel and Neumann functions, $h_l^+=j_l+in_l$, $\kappa=\epsilon^{1/2}$, ϵ is the energy of the electrons at the Fermi surface, the matrix T is the cluster t matrix[4]

$$T_{LL'}^{jj'}=\langle jL\,|\,(t^{-1}-B)^{-1}\,|\,j'L'\rangle \tag{6}$$

with, for convenience, the symbolical notation $T_{LL'}^{jj'}\equiv\langle jL\,|\,T\,|\,j'L'\rangle$ and where $t_l^j=-\sin\delta_l^j\exp(i\delta_l^j)$ with δ_l^j being a phase shift for the scatterer at $\vec{R}_j$, $B=-iG$, $G=J+iN$,

$$J_{LL'}^{jj'}=4\pi i^{l-l'}\sum_{L''}i^{l''}C_{LL'L''}j_{L''}(\vec{R}_{jj'})\ , \tag{7}$$

N follows from J by the replacement in (7) of $j_{L''}$ by $n_{L''}$ and $C_{LL'L''}$ are the Gaunt coefficients

$$C_{LL'L''}=\int d\hat{k}\,Y_L(\hat{k})Y_{L'}(\hat{k})Y_{L''}(\hat{k})\ .$$

Real spherical harmonics are used. This form is given because it shows clearly that in the scattered wave part proportional to the hankel function multiple scattering is accounted for in the cluster t matrix T.

All incoming waves proportional to the Bessel function add to $\exp[i\vec{k}\cdot(\vec{x}+\vec{R}_1)]$. The form (5) can be rewritten simply, such that it is valid also inside the muffin-tin sphere with radius $R_{\rm MT}$ of the ion at $\vec{R}_1$:

$$\psi_{\vec{k}}(\vec{x}+\vec{R}_1)=\frac{4\pi}{\Omega^{1/2}}\left[\sum_{\substack{L\\(l>l_{\max})}}j_L(\vec{x})\left[i^lY_L(\hat{k})\exp(i\vec{k}\cdot\vec{R}_1)+\sum_{j'L',j''L''}B_{LL'}^{1j'}T_{L'L''}^{j'j''}i^{l''}Y_{L''}(\hat{k})\exp(i\vec{k}\cdot\vec{R}_{j''})\right]\right.$$
$$\left.+\sum_{\substack{L\\(l\le l_{\max})}}\sum_{j'L'}R_L^1(\vec{x})\langle 1L\,|\,(1-Bt)^{-1}\,|\,j'L'\rangle i^{l'}Y_{L'}(\hat{k})\exp(i\vec{k}\cdot R_{j'})\right]\ . \tag{8}$$

One sees a part with $l>l_{\max}$ and a part with $l\le l_{\max}$, where $l_{\max}$ is the maximum angular momentum which contributes to the scattering. Owing to the gradient in the matrix element determining the wind force (1) one term of the $l>l_{\max}$ part contributes, namely the $l=l_{\max}+1$ term. The regular solution of the Schrödinger equation for the ion at $\vec{R}_1$ is, for $x\ge R_{\rm MT}$, equal to

$$R_l^1(x)=j_l(\kappa x)-it_l^1h_l^+(\kappa x)\quad(x\ge R_{\rm MT})\ . \tag{9}$$

Expression (1) for the wind force can be elaborated in a straightforward fashion with the use of the following equality for the volume integral

$$\int d^3x\,R_{L'}^*(\vec{x})[\vec{\nabla}v(\vec{x})]R_L(\vec{x})=R_{\rm MT}^2\int d\hat{x}[R_{L'}^*(\vec{x}),\vec{\nabla}R_L(\vec{x})]_{x=R_{\rm MT}}\ . \tag{10}$$

One finds for the $l_{\max}=0$ case

$$\vec{F}_{\rm wind}=\frac{4\kappa^2eE\tau}{\pi m}{\rm Im}\left[\tfrac{1}{3}T^{11}\hat{E}+\sum_{j\ne1}\left[\frac{j_1(\kappa R_{1j})}{\kappa R_{1j}}\hat{E}-j_2(\kappa R_{1j})(\hat{E}\cdot\hat{R}_{1j})\hat{R}_{1j}\right]T^{1j}\right.$$
$$\left.-i\sum_{\substack{jj'j''\\(j\ne1,j'\ne j'')}}h_1^-(\kappa R_{1j})j_1(\kappa R_{j'j''})(\hat{E}\cdot\hat{R}_{j'j''})\hat{R}_{1j}T^{jj'*}T^{1j''}\right]\ . \tag{11}$$

The angular-momentum indices for the matrix T have been omitted since they take only the value 0. Expression (11) has been calculated numerically for the different model situations apart from the factor $eE\tau/m$, which is the drift velocity.

For sake of comparison with results obtained previously with approximate expressions we derive a t-matrix improvement of the Born approximation (BA). Usually one replaces the potential matrix elements in the BA expression by t-matrix elements. We will proceed the other way around, by approximating the exact expression (11). A t-matrix BA expression for the wave function can be obtained from (5) by the replacement

$$T_{LL'}^{jj'}\to t_l^j\delta_{jj'}\delta_{LL'}\ . \tag{12}$$

This leads to a corresponding BA expression from (8), in which an additional replacement is induced

by (12)

$$(1-Bt)^{-1}\rightarrow 1+Bt\ . \tag{13}$$

As for the Bt term which follows from (13), the full regular solution $R_L^1(\vec{x})$ in (8) should be replaced by $j_L(\vec{x})$. All these replacements together imply that in expression (11) for the force in the first and third terms (12) should be used, while effectively in the second term

$$T^{1j}\rightarrow -ih_0^+(\kappa R_{1j})t^1t^j\ . \tag{14}$$

If one elaborates the Im operation in the expression obtained in this way the terms proportional to n_0 and n_1 are for small phase shifts cubic in η, while the other terms are quadratic. In an expression derived in the Born approximation cubic terms are not present. By omitting the Neumann-function terms the BA expressions converge and are even continuous in the limit $R_{1j}\rightarrow 0$. If these terms would be retained the BA t-matrix formula would lead to a singularity in the limit of vanishing distance between two scatterers. So the t-matrix BA formula for the wind force follows from (11) with (12) and (14) applied as indicated above and after omission of the Neumann function terms

$$\vec{F}_{\text{wind}}^{\text{BA}}=\frac{4\kappa^2eE\tau}{\pi m}\text{Im}\left[\tfrac{1}{3}t^1\hat{E}-\sum_{j\neq 1}\left[\frac{j_1(\kappa R_{1j})}{\kappa R_{1j}}\hat{E}-j_2(\kappa R_{1j})(\hat{E}\cdot\hat{R}_{1j})\hat{R}_{1j}\right]ij_0(\kappa R_{1j})t^1t^j\right.$$
$$\left.+\,i\sum_{j\neq 1}j_1^2(\kappa R_{1j})(\hat{E}\cdot\hat{R}_{1j})\hat{R}_{1j}t^1t^{j^*}\right]. \tag{15}$$

This expression still contains terms of order higher than quadratic in $\sin\delta$ and terms with factors $\cos\delta$. In an expression written down starting from BA such terms are not present. That is why in practice we used the following reduced form for the component of the t-matrix BA wind force in the direction of the electric field:

$$\vec{F}_{\text{wind}}^{\text{BA}}\cdot\hat{E}=-\frac{4\kappa^2eE\tau}{\pi m}\left[\tfrac{1}{3}\sin^2\delta^1+\sum_{j\neq 1}\sin\delta^1\sin\delta^j\right.$$
$$\left.\times\left[j_0(\kappa R_{1j})\frac{j_1(\kappa R_{1j})}{\kappa R_{1j}}-(\hat{E}\cdot\hat{R}_{1j})^2[j_0(\kappa R_{1j})j_2(\kappa R_{1j})+j_1^2(\kappa R_{1j})]\right]\right]. \tag{16}$$

An equivalent expression has been used previously[2,6] although in a restricted sense. In the case of vacancy scattering the vacancy phase shifts were taken equal to minus the atom phase shifts according to the rules to obtain Born phase shifts. In fact one finds, if one calculates the true scattering phase shifts for a vacancy, that this procedure is not correct. We will return to this point in the discussion of the results.

III. MODEL SITUATIONS

In the present paper we study the wind force acting on an ion in a fcc metal while it migrates from a cubic corner towards a vacancy at a face center. Therefore, we are dealing with a vacancy migration problem in a metal. In pseudopotential calculations[2,6] one uses a "subtracted model" (SM) as far as the scattering is concerned. This means, as it can be seen from the symbolical one-dimensional picture in Fig. 1, that the vacancy migration problem reduces to a 3-scatterers problem as soon as the migrating atom has started to move from its position at the cubic corner. It is, in fact, a vacancy-atom-vacancy problem. It will be clear that such an approach can only be expected to be valid for simple metals, in which case a BA or t-matrix BA treatment of the scattering is not too bad an approximation. A SM calculation using (11) makes only sense for not too strong scatterers although that expression treats scattering to all orders. The model itself is bound to be applicable for weaker scatterers. In addition it has to be realized that expression (11) is derived for nonoverlapping potentials, and it is clear that for realistic muffin-tin radii in the SM this is barely achieved when the atom is midway between cubic corner and face center. Nevertheless we applied (11) also for the SM, mainly for sake of comparison with t-matrix BA results obtained from (16).

In the finite-cluster model (FCM) the problem of

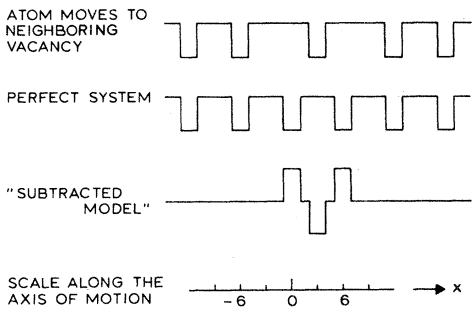

FIG. 1. One-dimensional picture of the subtracted model situation for vacancy migration, which leads to a 3-scatterer problem.

overlapping potentials does not arise. The metal is modeled by the migrating atom in its nearby environment (Fig. 2) and scattering is treated exactly. The approximation is that the extended bulk environment of the region where migration occurs is replaced by the constant interstitial potential, effectively by free space. The most complete nearby environment requires the treatment of scattering in a cluster of 19 scatterers. The simplest environment consists of 3 or 5 scatterers depending on one's preference. Since the electric field and, on the average, the electric current are chosen along the axis of motion one may expect a strong contribution from the two nearby atoms on this axis. On the other hand, the 5-scatterers case deals with those atoms which have equal distance to cubic corner and face center. In intermediate cases one counts 7, 11, and 15 scatterers as indicated in Fig. 2. Since no subtraction is applied the atom moves without overlap problems from the cubic corner, chosen as the origin, to the face center. The nearest-neighbor distance is chosen to be 6, being a reasonable value for a fcc metal.

In the present study, only s scattering is accounted for. Since this first study has more the character of looking for trends and of comparison with approximate methods used earlier we chose as potentials simple spherical wells. The well radius used mostly was 1.20 which allows for some range of validity of (11) for the SM midway between corner and face center (from 2.40 to 3.60). A few test calculations were made using a well radius of 0.15, for which case this range lies between 0.30 and 5.70. Further we chose the depth of the potential such that we studied a weak, a stronger, and a strong scatterer, having $\cot\delta_0$ equal to 10, 1, and 0.1, respectively.

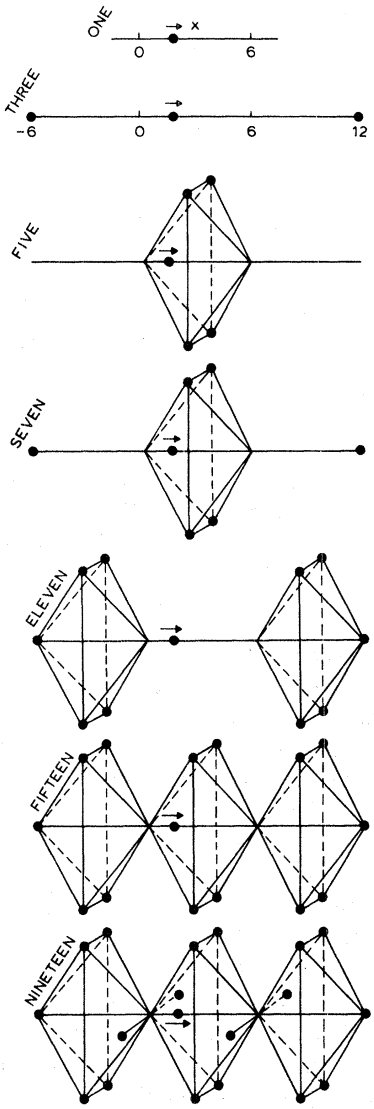

FIG. 2. Different cluster sizes and shapes used in the finite-cluster-model calculations. The atom migrates along the x axis, which connects a cubic corner and a nearest face center in a fcc metal. The nearest-neighbor distance is 6.

IV. RESULTS AND DISCUSSION

A. Subtracted model (SM)

The results for the subtracted model are given in Fig. 3. Figures 3(a)–3(c) apply for increasing scatterer strength given by $\cot\delta_0^{\text{atom}}=10$, 1, and 0.1, respectively. In order to show how far p and d scattering can be expected to be negligible $\cot\delta_l^{\text{atom}}$ for $l=1$ and 2 are printed after the value for

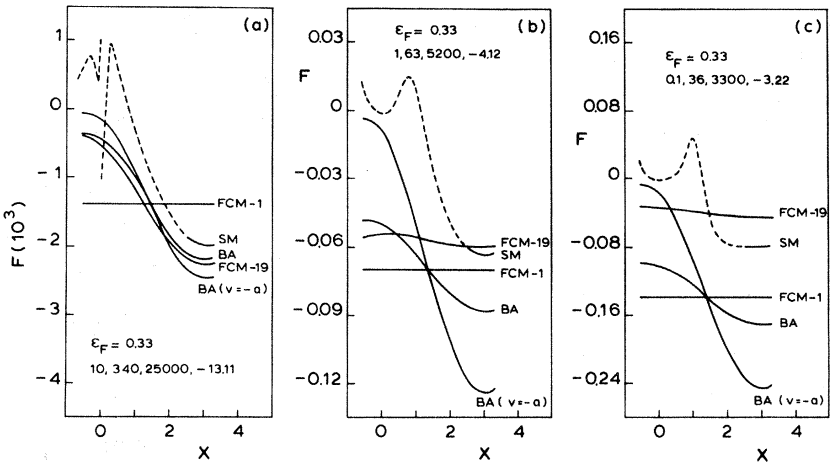

FIG. 3. Wind force as a function of the position of the migrating atom for a weak (a), a stronger (b), and a strong (c) scatterer, represented by $\cot\delta_0^{\text{atom}}=10$, 1, and 0.1, respectively. The numbers given under the Fermi energy are $\cot\delta_l^{\text{atom}}$ for $l=0$, 1, and 2 and $\cot\delta_0^{\text{vacancy}}$, respectively.

$cot\delta_0^{\text{atom}}$. It is seen that the d phase shift is negligibly small in all cases, while the p phase shift is still smaller than 0.03 rad if $\cot\delta_0^{\text{atom}}=0.1$. The $\cot\delta_0^{\text{vacancy}}$ apparently is larger than $-\cot\delta_0^{\text{atom}}$ for all cases, which implies that in the energy range of our calculations potential-well scattering is stronger than barrier scattering. The Fermi energy of 0.33 used is the free-electron value for a monovalent fcc metal with nearest-neighbor distance 6. The physical region of motion lies between $x=0$ and 6. Since the wind force as a function of the position is symmetrical with respect to the line $x=3$ just one value beyond $x=3$ is given. Further, the curves have been calculated for a few negative x values. The results corresponding to expressions (11) and (16) are indicated by SM and BA, respectively. In applying both expressions to the present model, the summation over j extends over the two vacancies in the three-center scattering complex. For comparison the FCM results for 1 scatterer and 19 scatterers are plotted also. The expression for 1 scatterer follows simply from (11) by omitting all terms except the one proportional to $T^{11}/3$, which factor has to be replaced by $t^1/3$. This case, of course, shows a position-independent force.

First it is seen that the BA result for the weakest scatterer follows the SM result closely. This is found particularly striking in a calculation we made for an even weaker scatterer with $\cos\delta_0^{\text{atom}}=100$. Further the FCM-19 result does not deviate much from the BA result for the energy 0.33, which corresponds to the case of a monovalent metal. There are deviations, however, between FCM-19 and BA results for the energies 0.53 and 0.70, which correspond to divalent and trivalent metals, respectively. (See Fig. 4.) Intuitively, one might expect that for weak scatterers the FCM results in the infinite-cluster limit should approach the BA result for the subtracted model. That this is not true can be seen readily from the weak scattering expression (16). In the SM the summation over j runs over the two values for the vacancy, and $\delta^j=-\delta^1$. In the FCM this summation runs over all lattice positions apart from the cubic corner and the face center while $\delta^j=\delta^1$. Clearly

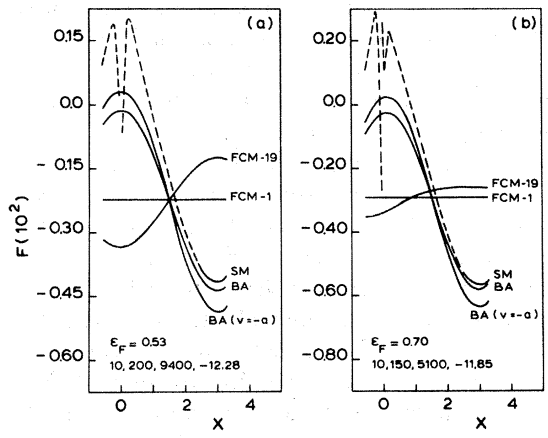

FIG. 4. Wind force as a function of the position of the migrating atom for a divalent ($\epsilon_F=0.53$) and a trivalent ($\epsilon_F=0.70$) metal. The numbers given under the Fermi energy are $\cot\delta_l^{\text{atom}}$ for $l=0$, 1, and 2, and $\cot\delta_0^{\text{vacancy}}$, respectively.

for weak scatterers the SM result follows from the corresponding FCM result after subtraction of a term which includes summation over the unperturbed lattice. The variation of the force over the path is therefore not represented correctly by the subtracted model. However, for weak scatterers, the contributions from the unperturbed lattice can be shown to have a spatial variation like $\sin\vec{G}\cdot\vec{R}_1$ where $\vec{G}$ is a reciprocal-lattice vector spanning the Fermi surface. The existence of such contributions from the unperturbed lattice was shown by Sorbello[2] in his pseudopotential calculations. The $\sin\vec{G}\cdot\vec{R}_1$ contributions only exist for polyvalent metals, and in any case, they play no role in electromigration since they vanish when averaged over the jump path. This explains why in Table I the average forces calculated from FCM-19 and BA for weak scatterers are not very different for $\epsilon=0.53$ or 0.70 despite the fact that the spatial variation of the FCM-19 and BA forces are very different.

In the region $x<2.40$ expression (11) is not valid if it is applied for the SM. That is why the SM curve is dashed in that region. The irregular behavior becomes dramatic near the origin. The value of the force according to (11) for the SM is finite. In fact only the h_1 term contributes and the divergence of the hankel function is canceled by the cluster t-matrix element factors which approach linearly to zero with R_{10}.

The t-matrix BA limit (16) has lost the irregularity in the region of overlap which is typical for the exact result according to (11). In the derivation of (15) it was already mentioned that in the lowest order BA limit Neumann function terms drop out. Reasoning the other way round one is here faced with an example that one can make errors if one tries to improve a treatment by merely replacing lowest order ingredients (potential matrix elements) by better ones (t-matrix elements) in a final expression. By omitting terms higher than quadratic in δ the replacement of terms quadratic in δ by t-matrix elements clearly is an inconsistent procedure.

Finally we want to draw attention to the fact that in the SM $\delta^{\text{vacancy}}\neq-\delta^{\text{atom}}$. We calculated

TABLE I. The average of the wind force over the path in units of the wind force for an isolated atom (FCM-1). The values are given for monovalent (0.33), divalent (0.53), and trivalent (0.70) metals, for the different model situations.

$\cot\delta_0^{\text{atom}}$		100	10	1	0.1
BA	$\epsilon=0.33$	1.037	1.029	1.013	1.011
	0.53	1.008	1.007	1.003	1.003
	0.70	0.978	0.981	0.990	0.990
BA($v=-a$)	$\epsilon=0.33$	1.038	1.038	1.038	1.038
	0.53	1.008	1.008	1.008	1.008
	0.70	0.978	0.978	0.978	0.978
FCM-3	$\epsilon=0.33$	1.024	1.037	0.941	0.769
	0.53	1.018	1.017	0.941	0.858
	0.70	0.973	0.973	0.946	0.889
FCM-5	$\epsilon=0.33$	0.919	0.885	0.812	0.548
	0.53	0.985	1.000	0.839	0.905
	0.70	1.045	1.043	0.880	1.100
FCM-7	$\epsilon=0.33$	0.944	0.928	0.762	0.350
	0.53	1.003	1.016	0.823	0.728
	0.70	1.018	1.017	0.808	0.933
FCM-11	$\epsilon=0.33$	1.155	1.178	1.015	0.689
	0.53	1.022	1.018	0.836	0.581
	0.70	0.957	0.950	0.771	0.435
FCM-15	$\epsilon=0.33$	1.073	1.058	0.857	0.404
	0.53	1.007	1.017	0.728	0.511
	0.70	1.002	0.995	0.631	0.443
FCM-19	$\epsilon=0.33$	1.112	1.109	0.817	0.293
	0.53	1.012	1.013	0.633	0.237
	0.70	0.987	0.971	0.526	0.272

also the t-matrix BA expression (16) using the equality. In Figs. 3 and 4 these results are indicated by BA ($v=-a$).

Figure 3(b) shows already a strong deviation from the correct BA result but also for the weak scatterer for different energies shown in Figs. 3(a) and 4, the BA($v=-a$) results move away from the exact SM results.

B. Finite-cluster model (FCM)

The FCM results are shown in Fig. 5. In the weak scatterer case [Fig. 5(a)] the curves for the three largest clusters follow each other closely, while the curves for the smaller clusters deviate markedly. It is seen that relative to the position-independent 1-atom line, the 3-atom and 5-atom curves add to the 7-atom curve and that similarly the 5-atom and 11-atom curves add to the 15-atom curve. From this additive behavior we conclude that multiple-scattering effects can still be neglected. This no longer holds for intermediate and strong scatterers as shown in Figs. 5(b) and 5(c). In general, but in particular for stronger scatterers, one does not expect that the 11-atom cluster will give meaningful results. For stronger scatterers the 5- and 7-atom clusters can be considered as more realistic small cluster representations of the more complete 15- and 19-atom clusters.

If the scatterers become stronger cancellation effects are observed due to the presence of an environment for almost all cluster sizes. By cancellation we mean that the wind force is reduced in comparison with the force experienced by one scatterer in free space, the FCM-1 case. Strong cancellation can occur for stronger scatterers, although we found that the effect depends on the Fermi energy which is used, on the valency of the host metal atoms.

This cancellation is seen most clearly from Table I in which for the various cases the average of the wind force over the path is given in units of the wind force for an isolated atom (FCM-1). Note that for weak scatterers the path averaged force is within a few percent of the FCM-1 force. This absence of an effect from the environment for weak scatterers is not a general feature for all potentials. For example, large cancellations (of order 50%) were obtained by Sorbello[6] in a weak-scattering calculation for some metals, but in those calculations the pseudopotentials employed gave appreciable p-wave scattering. In the s-wave scattering considered in the present work, large cancellation is associated with strong scatterers. The extent of the cancellation for strong scatterers is rather surprising.

The spatial variation of the wind force is noteworthy. For weak scatterers, the wind force exhibits sinusoidal-like variation about the FCM-1 value and is largest in magnitude near the "saddle point" of the path ($x=3$) and is considerably smaller in magnitude near the starting point ($x=0$). For strong scatterers, however, this behavior is not observed. We also remark that for all cases shown the average force over the path be-

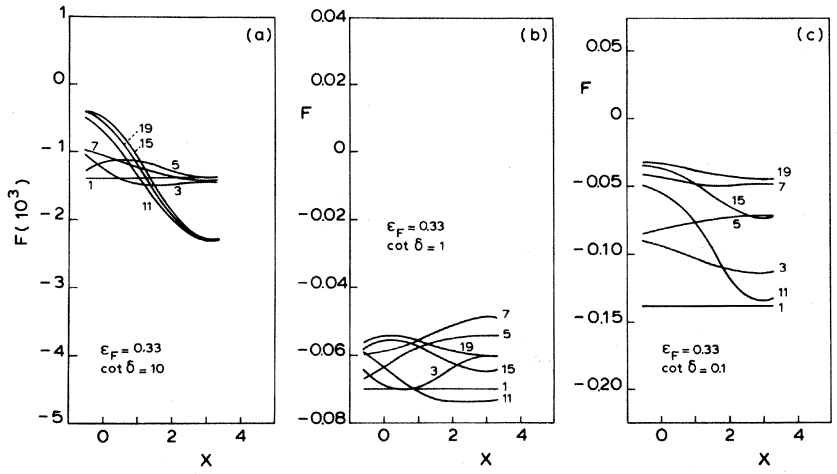

FIG. 5. Wind force as a function of the position of the migrating atom for different cluster sizes and three scatterer strengths. cotδ stands for $\cot\delta_0^{\text{atom}}$. The number indicating a curve stands for the number of scatterers corresponding to a cluster in the FCM.

tween $x=0$ and 6 is rather well approximated by the average of the forces at $x=0$ and 3. Such an approximation is sometimes made in electromigration calculations.[18] However, we hasten to add that some calculations we have made indicate that for strong scatterers this is not necessarily a good approximation. For example, when $\cot\delta=0.1$ and $\epsilon=0.53$ the procedure of approximating the path average force by the average of the forces at $x=0$ and 3 gives an error of about 30%.

V. CONCLUSIONS

Using a finite-cluster approach to electromigration we have presented the first multiple-scattering calculation of the electron wind force. All multiple-scattering effects are contained in the cluster T matrix appearing in expression (11). For strong scatterers, we find large cancellation effects in the wind force. These cancellations arise from contributions to the electron density due to the scattering of electrons by atoms in the neighborhood of the migrating atom. Our expression (11) can be generalized in a straightforward manner to include s-, p-, and d-wave scattering. Numerical calculations for a finite-cluster treatment of other defect complexes, such as those containing interstitial or substitutional impurities, are also possible. Further work is in progress.

[1]For reviews see: J. N. Pratt and R. G. R. Sellors, *Electrotransport in Metals and Alloys* (Trans. Techn. S. A. Riehen, Switzerland, 1973); H. B. Huntington, in *Diffusion in Solids: Recent Developments,* edited by A. S. Nowick and J. J. Burton (Academic, New York, 1974), p. 303; R. S. Sorbello, in *Electro- and Thermotransport in Metals and Alloys,* edited by R. E. Hummel and H. B. Huntington (The Metallurgical Society of American Institute of Metallurgical Engineers, New York, 1977).

[2]For a discussion of the most recent work see R. S. Sorbello, J. Phys. Chem. Solids 42, 309 (1981).

[3]H. B. Huntington and A. R. Grone, J. Phys. Chem. Solids 20, 76 (1961); V. B. Fiks, Fiz. Tverd. Tela (Leningrad) 1, 17 (1959) [Sov. Phys.—Solid State 1, 14 (1959)].

[4]For a discussion of the finite-cluster method see A. Lodder, J. Phys. F 6, 1885 (1976); 7, 139 (1977).

[5]C. Bosvieux and J. Friedel, J. Phys. Chem. Solids 23, 123 (1962).

[6]R. S. Sorbello, J. Phys. Chem. Solids 34, 937 (1973).

[7]D. Stroud, Phys. Rev. B 13, 4221 (1976).

[8]R. S. Sorbello, Phys. Status Solidi B 86, 671 (1978).

[9]R. S. Sorbello, Phys. Rev. B 15, 3045 (1977).

[10]W. L. Schaich, Phys. Rev. B 13, 3350 (1976).

[11]L. Sham, Phys. Rev. B 12, 3142 (1975).

[12]R. P. Feynman, Phys. Rev. 56, 340 (1939). For a discussion of the applicability of the Feynman-Hellmann theorem in electromigration see R. S. Sorbello and B. B. Dasgupta, Phys. Rev. B 21, 2196 (1980).

[13]T. C. Genoni and H. B. Huntington, Phys. Rev. B 16, 1344 (1977). These authors start with a somewhat more general form of Eq. (1) which allows them to go beyond an independent particle picture and include some nondiagonal aspects of electron screening. In their actual calculations, however, they revert to an expression equivalent to Eq. (1).

[14]See, for example, C. E. Van Dijkum and A. Lodder, Phys. Status Solidi B 106, 107 (1981).

[15]P. J. Braspenning and A. Lodder, J. Phys. F 11, 79 (1981).

[16]P. Kumar and R. S. Sorbello, Thin Solid Films 25, 25 (1975).

[17]P. R. Rimbey and R. S. Sorbello, Phys. Rev. B 21, 2150 (1980).

[18]M. Gerl, Z. Naturforsch. 26a, 1 (1971).